Analyst

FIELD INDUCED FRAGMENTATION SPECTRA FROM REACTIVE STAGE TANDEM DIFFERENTIAL MOBILITY SPECTROMETRY

Journal:	*Analyst*
Manuscript ID	AN-ART-04-2020-000665.R1
Article Type:	Paper
Date Submitted by the Author:	05-Jun-2020
Complete List of Authors:	Fowler, Peter; New Mexico State University, Chemistry and Biochemistry Pilgrim, Jacob ; New Mexico State University, Chemistry and Biochemistry Lee, Gyoung-il; New Mexico State University, Chemistry and Biochemistry Eiceman, Gary; New Mexico State University, Chemistry and Biochemistry; Loughborough Univ., Chemistry

ARTICLE Journal Name

FIELD INDUCED FRAGMENTATION SPECTRA FROM REACTIVE STAGE-TANDEM DIFFERENTIAL MOBILITY SPECTROMETRY

P.E. Fowler,*[a] J.Z. Pilgrim, [a] G. Lee [a] and G.A. Eiceman[a]

Received 00th January 20xx,
Accepted 00th January 20xx

DOI: 10.1039/x0xx00000x

A planar tandem differential mobility spectrometer was integrated with a middle reactive stage to fragment ions, mobility selected in a first analyzer stage using characteristic compensation and separation fields. Fragmentation occurred in air at ambient pressure of 660 torr (8.8 kPa) with electric fields of 10 to 35 kV/cm (E/N of 52 to 180 Td) between two 1 mm wide metal strips, located on each analyzer plate between the first and second mobility stages. Field induced fragmentation (FIF) spectra were produced by characterizing, in a last stage, the mobilities of fragment ions from protonated monomers of 43 oxygen-containing volatile organic compounds from five chemical classes. The extent of fragmentation was proportional to E/N with alcohols, aldehydes, and ethers undergoing multiples steps of fragmentation; acetates fragmented only to a single ion, protonated acetic acid. In contrast, fragmentation of ketones occurred only for methyl i-butyl ketone and 2-hexanone. Fragment ion identities were supported by mass-analysis and known fragmentation routes and suggested that field induced fragmentation at ambient pressure can introduce structural information into FIF spectra, establishing a foundation for chemical identification using mobility methods.

Key Words: reactive stage, tandem, differential mobility spectrometry, field induced fragmentation spectra, oxygen containing, volatile organic compounds.

Introduction

Ion mobility spectrometry (IMS) has received wide-spread acceptance since the 1980s for rapid in-field chemical measurements of substances with military or security interests.[1–3] Other applications of IMS have included the monitoring of airborne vapours in ambient air for volatile organic compounds,[4,5] the screening of food purity[6–8] and the clinical analysis of breath for diagnosis of human health.[9–11] These methods provide picogram detection limits and selective response from a combination of ionization chemistry at ambient pressure and ion characterization by mobility, often in portable technology[12][13][14] with low power demand and relatively simple drift tube designs.[12,15,16] Mobility spectra obtained with such analysers are commonly simple patterns of one or two ions derived from a substance and the resolving power for hand-held or portable instruments is commonly 15 to 30, although increases to ~60 have been described recently.[17] Nonetheless, little structural information can be found in mobility spectra from these instruments limiting IMS methodologies to the selective detection of trace amounts of substances. Mobility spectra broadly lack the detail or content which are necessary for molecular identification.

One IMS method, termed differential mobility spectrometry (DMS), was introduced in 2000 as a small, planar analyser with a 12 mm long stage for ion separation.[18] This analyser was preceded by larger embodiments, both planar[19] and cylindrical,[20] termed field asymmetric IMS (FAIMS). Later, analysers with micron-size mobility stages were introduced as ultraFAIMS.[21,22] Designs of DMS or FAIMS analysers are distinguished as ion filters, rather than spectrometers since flow into the mobility stage is continuous for ion characterization (and separation) through field-dependent, mobility behaviors.[22,23] Differential mobility analysers can be combined in series for sequential processing of ions[24] using the concept of tandem or multiple stages to reduce "chemical noise preferentially over analytical signal. The result is an increase in the signal-to-noise ratio and improved specificity of response, a concept described earlier for tandem mass spectrometry.[25,26] While this was demonstrated earlier in tandem DMS methods,[24] there was no increase in the amount of structural information in mobility spectra from sequential processing of ions. Structural information can be introduced into mobility spectra from ambient pressure mobility analysers when a precursor ion is isolated in a first mobility stage, fragmented in a reactive middle stage (using strong electric fields[27,28] or elevated temperatures[29,30]) and mobility analysed in a final mobility stage. Mobility spectra from this final mobility stage, including precursor and fragment ions, have been called field induced fragmentation (FIF) spectra,[31] and can be seen as mobility analogues to collision induced dissociation spectra from tandem mass spectrometry.

Ion fragmentation at ambient pressure has been observed for a range of chemical classes including aromatic hydrocarbons,[32] esters,[33] organophosphorus compounds,[34] and alcohols[35] in single DMS analysers with electric fields up to 30,000 V/cm. The location for electric field heating of ions may occur between the parallel plates or in fringe fields extending from the plates of the DMS analyser. Although there is no agreement on the exact location of fragmentation, protonated monomers of compounds from a range of functional groups have been fragmented from 100 to ~200 Td in air at ambient pressure. In other studies of ions in electric fields, negative chloride adducts of explosives[27] and protonated monomers of some oxygen-containing compounds[28] were decomposed in a wire grid assembly within a cylindrical drift tube. Although fragmentation was observed for $MH^+(H_2O)_n$ of alcohols at 129 Td through water elimination and of esters through six member ring rearrangement, field strengths were insufficient to fragment

[a.] Department of Chemistry and Biochemistry
[b.] New Mexico State University
[c.] Las Cruces, NM 88003
*Corresponding author contact email: geiceman@nmsu.edu

protonated monomers of ethers and aldehydes with their strained four member rings transition states. Even with alcohols and esters, only a single fragment ion (a carbocation) was observed in the wire grid assembly, in contrast to the multiple levels of fragmentation described at E/N of 129 Td with proton transfer reaction mass spectrometry of alcohols.[36] This difference in extent of fragmentation, though not fully explored, may be attributed provisionally to large inhomogeneities in electric fields of the wire grid structures and these may be reduced or eliminated in planar structures as found in a DMS analyser. Other structures to fragment ions in mobility devices have been reported, also without detailed descriptions or understandings.[37–39]

Objectives in this present study include i) the construction and demonstration of a tandem DMS with a middle reactive stage on the flat analyser plates, and ii) the collection and evaluation of FIF spectra from this planar reactive stage tandem DMS. Effort was given to assessing if successive levels of fragmentation occurred with a planar reactive stage and to supporting ion identification by mass-analysis. Oxygen-containing VOCs were selected from studies with a wire grid assembly (as reactive stage) in a cylindrical tandem drift tube[28,31] for limited comparisons of performance.

Experimental

Instrumentation

Gas Chromatograph- A model 5890 series II gas chromatograph (Hewlett-Packard Corp, Avondale, PA) was equipped with a split-splitless injector, a 0.25 µm DB-5 capillary column (15 m long X 0.2 mm ID, Agilent Technologies Inc., Santa Clara, CA), and a reactive stage tandem differential mobility spectrometer as detector. The analytical column was joined, using Vu2 Union® Connectors (Restek Corp, Bellefonte, PA), to a 25 cm long transfer line, an aluminium clad SGE HT5 capillary column (0.32 mm ID, 0.1 µm film) from Millipore Sigma (St. Louis, MO) kept at 180°C. A make-up flow for column effluent was 1 L/min of air purified through 13x molecular sieve to a moisture of 1 ± 0.5 ppm and monitored using a Moisture Image Series 2 (GE Panametrics, Inc. Waltham, MA). Flow was controlled using mass flow controllers, model 810C-DR-2-VI-SO (Sierra Instruments, Inc. Monterey, CA). Carrier gas for the gas chromatographic column was nitrogen and was purified through in house designed scrubber containing 5Å molecular sieve and an oxygen/moisture trap Model No: OT3-2 (Agilent Technologies, Santa Clara, CA).

Reactive Stage Tandem Differential Mobility Spectrometer- The tandem DMS was made of two plates (Figure 1) separated by a 0.5 mm Teflon gasket and held under compression in an aluminium frame (Fig. 1S, Supplemental Material). The plates were metal-bonded ceramic (REMTEC, Norwood, MA) with 8 mm long x 5 wide mm analyser stages, a 1 mm long x 5 mm wide reactive stage, and 4 mm long x 5 mm wide Faraday plate detectors. The ion source was a 2 mCi Ni-63 foil placed inside a modified stainless-steel union (Swagelok Co., El Paso, TX) attached to the frame holding the plates. Each DMS stage was controlled using custom software and electronics adapted from a hand-held DMS called JUNO (ChemRing Sensors and Electronic Systems, Charlotte, NC, USA). Operating parameters of the tandem DMS were: gas temperature at inlet, 55±1°C; pressure, 660 torr (8.8 kPa) or number density (N, 1.94 x 10^{19} molecules/cm^3 at 54°C); and linear velocity of gas flow through the tandem DMS, 6.7 m/s/. A temperature gradient in the body of the analyser was 5°C. One strip of the reactive stage was provided a symmetric waveform at 4.19 MHz and with amplitudes of 1 to 3.5 kV (52 to 180 Td) using electronics from GAA Custom Electronics (Kennewick, WA) and the second strip of the reactive stage was ground potential. Power for the reactive stage ranged from 0.4 to 13.4 W for 26 to 155 Td, respectively (see Table 2S in Supplemental Material).

GC-Tandem DMS/MS- A second tandem DMS drift tube without Faraday plate detectors was attached to a model 5890 series II gas chromatograph (Hewlett-Packard, Co., Avondale, PA) as described above. Ions in purified air were drawn at 1 L/min through the DMS analyser and into the capillary inlet (80°C) of a model 2010 mass spectrometer (Shimadzu Corp., Kyoto, Japan) for mass analysis of ions. Conditions for mass analysis were: range, m/z 25 to 400; scan speed, 125 amu/s; capillary inlet temperature, 50°C; electron multiplier voltage, 2.6 kV; and MS analyser vacuum, 1.0 x 10^{-5} torr.

Chemicals and Reagents

A chemical standard, 2,6 di-tert-butyl pyridine, and 45 volatile organic compounds (Table 1) were obtained from Millipore-Sigma Chemical Co. (St. Louis, MO) at 97% purity or better. Stock solutions were prepared in dichloromethane (99.7% purity, Alfa Aesar, Tewksbury, MA) at 5 to 100 ng/µL per compound. A calibration solution of 1-butanol, 2-hexanone, heptyl acetate, octanal, and 2,6 di-tert-butyl pyridine with each at 100 ng/uL, was prepared daily by dilution in CH_2Cl_2 from a neat mixture.

Procedures

General procedures- Measurements were made using 1 µL injections in splitless mode with purge on at 30 s. Conditions for chromatographic analysis were: injection port, 180°C; initial temperature, 40°C; final temperature, 180°C; and temperature program rate, 8°C/min. Spectra from the reactive stage tandem DMS were obtained for three modes (separation field or voltage was kept constant on both DMS stages in all experiments at 46.4 Td (18,000 V/cm).

i) single stage scanning where DMS1 and the reactive stage were inactive and DMS2 was scanned in compensation voltage from -30 to +10 V (3.1 to 1.03 Td).

ii) mobility isolation of an ion peak where the reactive stage was inactive and DMS1 was set to specific compensation voltages characteristic of particular ions then passed to DMS2 with scanned for compensation voltage,

iii) collection of FIF spectra where DMS1 was used to mobility isolate an ion at characteristic and fixed compensation voltage, the reactive stage was active at some value for E/N, and DMS2 was scanned in compensation voltage.

Mass Analysis of Ions- Fragment ions were mass-analysed using the GC-tandem DMS-MS instrument in two modes of operation. In a first mode, all stages of the tandem DMS were inactive without any

filtering. In a second mode, the mobility stages were controlled to mobility-isolate an ion. Mass spectra could be obtained in both modes with the reactive stage active or inactive.

Specific Procedures

Two procedures were used to insure comparability of findings over the study period based on concerns for stability of the technology and of the experimental conditions.

1. Dispersion plots were obtained daily for the reactant ion peak (RIP) by scanning separation voltages 600 to 1500 V (30.9 to 77.26 Td). No solvent or sample was used for these dispersion plots. Plots were examined for the appearance of impurities or variations in performance.

2. The calibration standard was characterized daily using one microliter of solution using mode i) described above and response was compared to a record of ion peak intensity, compensation voltage, and chromatographic efficiency.

Studies on fragmentation by E/N in the reactive stage were made only when consistency of experimental conditions and technology has been assured by these measurement controls.

3. Spectra were obtained for members of the aldehyde mixture from analysis by GC-tandem DMS using methods i) to iii), described above.

4. Spectra were obtained for n-hexanal as the waveform amplitude on the reactive stage was increased in 8 steps of 0, 93, 103, 113, 124, 134, 144, and 155 Td.

Data Processing and Presentation

Data sets from measurements by GC-reactive stage tandem DMS were processed in Origin (OriginLab Corp) and Excel 2016 (MicroSoft Corp) to obtain spectra, topographic plots, and peak areas by Gaussian fitting. Results from mass analysis of ions were processed using Shimadzu software to extract into Excel values for ion mass and intensities. In graphics and discussion below, voltages of instrument parameters are used for best representation of experimental conditions and number density normalized fields (E/N) are shown for convenient interlaboratory comparison. The conversion from V to E (V/cm) was V/0.05 cm, from E to E/N at 660 torr (8.8 kPa) and 55°C was (E/1.94 x 10^{19} cm^{-3}) V/cm^2 and conversion to Td was E/(1 x 10^{-17} V/cm^2).

Results and Discussion

DMS Spectra and Mobility Isolation of Protonated Monomers for Aldehydes

Results from analysis of a mixture of n-aldehydes (butanal to nonanal) using gas chromatography with the tandem DMS as detector are shown in Figure 2 as a plot of ion intensity, chromatographic retention time, and DMS compensation voltage (field). The first DMS stage (DMS1) and the reactive stage were both inactive in this measurement and ions were mobility characterized in the second DMS stage (DMS2) making the measurement equivalent to analysis using a single stage DMS.[18,23] The reactant ion is $H^+(H_2O)_n$ with a beta emitter (^{63}Ni foil) in purified air and a reactant ion peak (RIP) is seen at a compensation voltage of -7 V. Intensity of the RIP is constant throughout the measurement except during the elution of an aldehyde (M) into the ion source were M reacts with $H^+(H_2O)_n$ forming a product ion or protonated monomer ($MH^+(H_2O)_n$). These have characteristic compensation voltages (CV) within the homologous series of aldehydes as marked in Figure 2. At vapor concentrations used here, another product ion, the proton bound dimer (M_2H^+), forms from the association of M with $MH^+(H_2O)_n$, also marked in Figure 2. An example is seen for n-butanal with an elution time of 375 s and CV values of -4 V for the protonated monomer and -0.8 V for the proton bound dimer. As a homologous series increases in mass, with successive increases in carbon number, CV values for protonated monomers trend stepwise in the direction of 0 V, reaching -0.5 V for n-nonanal. This pattern is consistent with trends in CV and mass documented first for a homologous series of ketones.[40] Compensation voltages of proton bound dimers also undergo stepwise displacement toward 0 V with increases in carbon numbers, although the increments are small compared to protonated monomers, as observed previously.[40] Consequently, resolution decreases between pairs of peaks ($MH^+(H_2O)_n$ and M_2H^+) from 4.3 for n-butanal to 0.4 for n-nonanal. This is seen as partial convolution of peaks in Figure 2.

All product ions were mobility-isolated completely from the RIP in DMS 1 with a separation voltage of 900 V (46 Td) and protonated monomers could be isolated from proton bound dimers with no or minor ion leakage. This was <10% of original peak intensity for proton bound dimers from n-butanal to n-heptanal (Figure 2S, Supplemental Material). While the effectiveness in isolating protonated monomers of n-octanal and n-nonanal were thought similar to n-heptanal, a definitive determination is prevented by convolution with proton bound dimer (Fig. 2). Isolation could be improved with narrow CV ranges on the shoulder of the protonated monomer with a loss of ion flux into the reactive stage, the next step in sequential processing of ions. In studies on ion fragmentation described below, the minor amounts of proton bound dimer passing inadvertently into the reactive stage were considered negligible in view of the comparatively low reactivity of proton bound dimers in field induced fragmentation.[33,36] Similar patterns in retention times, compensation voltages, and patterns of resolution for protonated monomers and proton bound dimers were observed with other oxygen-containing volatile organic compounds and a list of CV values is given in Table 1.

Fragmentation of Mobility Isolated Protonated Monomers

When protonated monomers of n-aldehydes were isolated from the RIP and proton bound dimers and passed into a reactive stage at 129 Td, intensities for $MH^+(H_2O)_n$ of each aldehyde were depleted and replaced with a fragment ion peak at slightly larger negative CV values (Figure 3). These intense peaks appeared at the same retention times as, and at compensation voltages near, the protonated monomers (represented as green shaded ellipses in Fig. 3). The fragments were formed by field induced fragmentation in the reactive stage through a rearrangement reaction with a strained four-member ring transition state (TS, Eq. 1). Thus, the intense ions

in Fig. 3 arose from field induced heating of ions with bond migration and dehydration to an unsaturated carbocation, $C_4H_7^+$ for n-butanal (Eq. 2):[41,42]

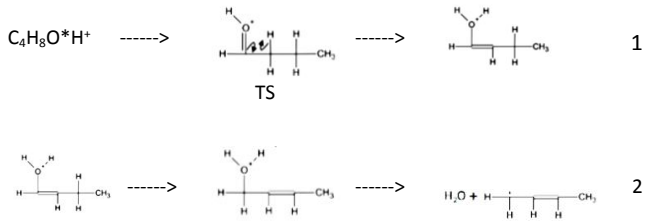

1

2

The patterns of these fragment ions in Figure 3 suggest complete fragmentation at 129 Td for protonated monomers from n-butanal to n-heptanal. Measures for completeness of fragmentation for n-octanal and n-nonanal since peaks convolve for protonated monomer and fragment ion.

Ion energies in the reactive stage were increased by multiples of 1.76, 2.37, and 3.13 for 93, 124, and 155 Td, respectively over thermal energy of $6.8x10^{-21}$ J/molecule. These increases were calculated using centre of mass kinetic energies and compared to a multiple of 2 at 129 Td in wire grids.[31] Fragmentation of ions occurred within a volume at the 1 mm reactive stage (metal strip, Fig. 1). Ion residence time would be 150 µs (629 oscillations) using simply this mechanical dimension. Fringe fields extending 1 mm on either side of the strip (see Figure 3S, Supplemental Material) could result in ion residence times of 450 µs and 1886 oscillations. Likely, residences times and oscillations are bounded between these extremes.

In addition to the intense peaks in Fig. 3 (the unsaturated carbocation fragment, $C_nH_{2n-1}^+$), other ions with lesser intensity were observed at CV of -6.0 V for n-hexanal and n-heptanal and -3.8 V for n-octanal and n-nonanal. These were attributed to the decomposition of the unsaturated carbocations with a second level of fragmentation and neutral loss of C_2H_4 for n-hexanal and C_3H_6 for n-heptanal to $C_4H_7^+$. Mass-analyses for n-octanal and n-nonanal showed secondary neutral loss of C_3H_6 for n-octanol and C_4H_8 for n-nonanal to $C_5H_9^+$, consistent with prior studies by mass spectrometry.[41,42] This pattern of a primary fragment ion with high intensity and ions at low intensities from a second level of fragmentation was observed also for ethers and for alcohols, consistent with both DMS[35] and MS investigations.[36] Acetates exhibited near quantitative decomposition to a single fragment ion, protonated acetic acid ($C_2H_3OH^+$)[33,43] and ketones showed significant fragmentation for only methyl i-butyl ketone contrasting with vacuum-based mass spectrometry where multi-step decompositions were observed.[44] While fragmentation here was considered limited in contrast to observations in mass spectrometry, the production of second and sometimes third levels of fragmentation had not been observed with wire grid assemblies in cylindrical drift tubes.[27,28]

Fragmentation as a function of E/N

The production of second and third levels of fragmentation described above with the reactive stage tandem DMS analyser demonstrated that the planar reactive stage produced more extensive fragmentation than a wire grid assembly in cylindrical drift tube.[28,31] The extent of fragmentation was explored further using a range of electric fields from 0 to 155 Td in the reactive stage and shown in Figure 4 with field induced fragmentation (FIF) spectra for a representative compound, n-hexanal. In the FIF spectrum at 0 Td, the intense ion peak at -2V is a hydrated protonated monomer (n = 1,2) and the neighbouring peak at ~0 V is the proton bound dimer. There is no detectable fragment ion intensity at -3 to -8 V for E/N values of 0 or 93 Td, though a decrease in signal strength occurs (Table 2) due to losses in ion transmission with planar structures with increased E/N. This loss in intensity continues generally from losses in transmission efficiency as E/N is increased to 155 Td, though losses in transmission efficiency are greater for protonated monomers and small ions of fragments than for the proton bound dimer.

At E/N of 103 Td, a shoulder on the protonated monomer peak can be observed at -3 V and is understood to arise from a first level of fragmentation to the unsaturated carbocation (as in Eqs. 1 and 2). At 113 Td, losses in ion abundance are nearly 90% for the protonated monomer and 85% for the proton bound dimer with the growth in fragment ion abundance. This intense fragment ion peak is $C_nH_{2n-1}^+$, as seen in Figure 3 for n-hexanal and other aldehydes.

Changes in ion abundance from 103 to 113 Td show a near conservation of charge with losses of 4% for M_2H^+ and 27% for $MH^+(H_2O)_n$ against an increase of 28% for the fragment ion (from 17% to 45%). Despite limitations in calculating conservation of charge with planar DMS analysers, the loss of only ~2% for total ions was permitted by the small difference of 10 Td in reactive stage field.

A next major development occurs at 124 Td (Fig. 4) when a second level of fragmentation for n-hexanal become evident with an ion at CV of -6 V. This ion was mass analysed as $C_4H_7^+$ and could arise from a concerted or stepwise reaction derived from the first fragment $C_nH_{2n-1}^+$ with loss of an ethene neutral, as in Equation 3:

$$C_6H_{11}^+ \quad \text{------>} \quad C_2H_4 \quad + \quad C_4H_7^+ \qquad 3$$

This was observed also for n-heptanal in contrast to n-octanal and n-nonanal where $C_5H_9^+$ was produced. Further increases in E/N resulted in decreases in relative abundances of unsaturated carbocations and increases in $C_4H_7^+$ although poor transmission coefficients for $C_4H_7^+$ will under-report actual fragmentation yields. Support for this stepwise fragmentation with increased E/N can be found in studies by proton transfer reaction mass spectrometry[36] where protonated alcohols underwent fragmentation successively to smaller ions. Although details of fragmentation and successive levels of fragment ion formation for n-hexanal with increased E/N are shown as an example, similar patterns were observed for other aldehydes and alcohols consistent with literature reports using mass spectrometry.[41–44] While some aspects of fragmentation could be understood as general to compounds in Table 1 and patterns of FIF spectra exhibited similarities within a chemical family, differences existed between functional groups.

Patterns of Ion Fragments in FIF Spectra of Oxygen-Containing VOCs

Compensation voltages for ion fragments of substances within and between chemical families were plotted versus carbon number as shown for aldehydes in Figure 5 and for alcohols in Figure 6.

Compensation voltages for protonated monomers of aldehydes (circles, Fig. 5) match those seen in Figure 3. Fragments from the first level of fragmentation (to unsaturated carbocations) are shown as triangles and a second level of fragmentation with loss of an alkene neutral to alkyl ions (either $C_4H_7^+$ or $C_5H_9^+$,) is shown as squares in Fig. 5. Specifically, water elimination from MH^+ by rearrangement was the first step of fragmentation for n-butanal to n-nonanal producing an ion with general formula $C_nH_{2n-1}^+$ (triangle symbols). In a second step of fragmentation, n-hexanal and n-heptanal produce $C_4H_7^+$ while n-octanal and n-nonanal form $C_5H_9^+$ as consistent with mass analysis described in the next section. At this E/N (129 Td), third levels of fragmentation were not observed for aldehydes.

Plots for alcohols (Fig. 6) show trends which roughly parallel those in aldehydes although simple water elimination to a saturated carbocation is the first level of fragmentation. The carbocation is rapidly fragmented to second and third levels of fragmentation and is not observed at this E/N. Rather, only the second and third levels of fragmentation form favoured ions which are dependent on carbon number (triangles). A third step of fragmentation (diamonds) was observed for n-hexanol to n-nonanol. Similar findings for the formation of first and second steps in the fragmentation of 1-propanol and 1-butanol have been reported.[45]

Only a first level of fragmentation by rearrangement to a protonated acetic acid was observed for protonated monomers of acetates, clearly described in DMS[33] and MS.[41,43] Fragmentation with ethers to a common ion was seen (Table 1S, Supplemental Materials) which differs from findings with a wire grid assembly where little or no fragmentation was observed at 129 Td.[31] In contrast, ketones were not fragmented in either design.

Compensation voltages of the smallest ion fragments observed in FIF spectra for alcohols, acetates, aldehydes, and ethers are plotted in Figure 7 and trends suggest the existence of small ions which are common within each chemical family. Simultaneously, the patterns of CV values for ions within a class differed from other classes and provide a foundation to distinguish particular chemical functional groups by moieties. This conclusion is consistent with observations of mobility spectra from a single stage drift tube instrument where class-specific fragment ions were apparently learned by neural networks.[46] Such ions were thought to arise from in-source fragmentation through charge exchange reactions with high energy reactant ion intermediates ($N_4^{+\cdot}$, $H_2O^{+\cdot}$) following beta discharge into air or nitrogen at ambient pressure. Plots similar to Figure 7 were made from drift tube spectra,[46] though never published lacking mass-analysis of ions.

Mass Analysis of Ions using GC Tandem DMS/MS

Product ions and ions attributable to fragmentation in the reactive stage were mass analysed using the GC tandem DMS MS instrument and are summarized in Table 3. Both DMS stages were inactive and mass spectra included proton bound dimers, protonated monomers, and fragment ions and identifications in Table 3 were based on mass-analysis with known chemistry of ionization and pathways for fragmentation.[41–44] Ion abundances in Table 3 included background subtraction of intensities from fragment ion formed in the interface between the atmospheric pressure and vacuum of the mass spectrometer. This unwanted fragmentation could not be reduced significantly using potential drops in the Q-array of the Shimadzu 2010 mass spectrometer. Intensities given in Table 3 were determined from a combination of the appearance of new ions and of the changes in the percentage of abundance in mass spectra, between an active versus inactive reactive stage. In some instances, the background ion intensities in the interface prevented reliable determination of ion masses. The summary given in Table 3 thus is an incomplete measure of all ions formed in the reactive stage and contains ions of only comparatively high intensity. Ions of minor intensity in the tandem DMS were also mass-analysed and were consistent with known fragmentation reactions in vacuum based studies[36,41–44] and some prior DMS-based mass analysis.[32,33,35] Results in Table 3 do not include ethers which were too low intensity for mass analysis (see Table 2S in Supplemental Material)

Finally, protonated monomers for ketones did not fragment (apart from MIBK) at any E/N and mass analysis for ketones (Table 2S) confirms the identities of protonated monomer and proton bound dimer.

Conclusions

A tandem DMS, modified with a middle reactive stage, produced field induced fragmentation spectra with ions distinctive of oxygen containing volatile organic compounds within a chemical class and consistent with accepted pathways of fragmentation and mass analysis of abundant ions. Differences in class-wide fragment ions among chemical families should enable advances in spectral interpretation at ambient pressure in ways that mirror vacuum based collision induced dissociation spectra with tandem mass spectrometry. Fragmentation of mobility selected ions when matured in tandem DMS instruments may provide a capability to assign spectra to chemical classes as observed for in-source fragmentation in IMS.[46] The extent of fragmentation was adjustable using the electric field strength in the reactive stage providing a basis for additional control in the concept of sequential ion processing in tandem or multi-stage mobility analysers. Extension of these capabilities to compounds from a wide selection of substances and moieties will be necessary to bring a fuller assessment of the concept of reactive stage tandem differential mobility spectrometry.

Conflicts of interest

There are no conflicts to declare.

Acknowledgements

Support by the National Science Foundation under Award No. IIP-1827525, by the New Mexico Space Grant Consortium to P.E. Fowler, and by Chemring Sensors and Electronic Systems with control electronics and software is gratefully acknowledged.

Notes and references

1 J. Puton and J. Namieśnik, *TrAC Trends Anal. Chem.*, , DOI:10.1016/j.trac.2016.06.002.

2 T. Satoh, S. Kishi, H. Nagashima, M. Tachikawa, M. Kanamori-Kataoka, T. Nakagawa, N. Kitagawa, K. Tokita, S. Yamamoto and Y. Seto, *Anal. Chim. Acta*, 2015, **865**, 39–52.

3 D. D. Fetterolf and T. D. Clark, *J. Forensic Sci.*, 1993, **38**, 13373J.

4 T. Limero, *SAE Tech. Pap.*, , DOI:10.4271/2007-01-3220.

5 T. Limero, E. Reese, P. Cheng and J. Trowbridge, *Int. J. Ion Mobil. Spectrom.*, 2011, **14**, 81–91.

6 M. del M. Contreras, N. Arroyo-Manzanares, C. Arce and L. Arce, *Food Control*, 2019, **98**, 82–93.

7 D. Cavanna, S. Zanardi, C. Dall'Asta and M. Suman, *Food Chem.*, 2019, **271**, 691–696.

8 M. Hernández-Mesa, D. Ropartz, A. M. García-Campaña, H. Rogniaux, G. Dervilly-Pinel and B. Le Bizec, *Molecules*, 2019, **24**, 1–28.

9 H. Handa, A. Usuba, S. Maddula, J. I. Baumbach, M. Mineshita and T. Miyazawa, *PLoS One*, 2014, **9**, e114555.

10 M. Basanta, R. M. Jarvis, Y. Xu, G. Blackburn, R. Tal-Singer, A. Woodcock, D. Singh, R. Goodacre, C. L. P. Thomas and S. J. Fowler, *Analyst*, 2010, **135**, 315–20.

11 E. Brodrick, A. Davies, P. Neill, L. Hanna and E. M. Williams, *J. Breath Res.*, , DOI:10.1088/1752-7155/9/2/027109.

12 R. B. Turner and J. L. Brokenshire, *Trends Anal. Chem.*, 1994, **13**, 275–280.

13 A. P. Snyder, C. S. Harden, A. H. Brittain, M. Kim, N. S. Arnold and H. L. C. Meuzelaar, *Anal.Chem.*, 1993, 299–306.

14 J. S. Babis, R. P. Sperline, A. K. Knight, D. A. Jones, C. A. Gresham and M. B. Denton, *Anal. Bioanal. Chem.*, 2009, **395**, 411–419.

15 T. Reinecke and B. H. Clowers, *HardwareX*, , DOI:10.1016/j.ohx.2018.e00030.

16 R. Cumeras, E. Figueras, C. E. Davis, J. I. Baumbach and I. Gràcia, *Analyst*, 2015, **140**, 1376–1390.

17 A. Ahrens, M. Hitzemann and S. Zimmermann, *Int. J. Ion Mobil. Spectrom.*, 2019, **22**, 77–83.

18 R. A. Miller, G. A. Eiceman, E. G. Nazarov and A. T. King, *Sensors Actuators, B Chem.*, , DOI:10.1016/S0925-4005(00)00535-9.

19 I. A. Buryakov, E. V. Krylov, E. G. Nazarov and U. K. Rasulev, *Int. J. Mass Spectrom. Ion Process.*, 1993, **128**, 143–148.

20 R. W. Purves, R. Guevremont, S. Day, C. W. Pipich and M. S. Matyjaszczyk, *Rev. Sci. Instrum.*, 1998, **69**, 4094–4105.

21 A. A. Shvartsburg, K. Tang, R. D. Smith, M. Holden, M. Rush, A. Thompson and D. Toutoungi, *Anal. Chem.*, 2009, **81**, 8048–8053.

22 K. M. M. Kabir and W. A. Donald, *TrAC - Trends Anal. Chem.*, 2017, **97**, 399–427.

23 B. M. Kolakowski and Z. Mester, *Analyst*, 2007, **132**, 842–864.

24 M. R. Menlyadiev and G. A. Eiceman, *Anal. Chem.*, 2014, **86**, 2395–2402.

25 R. A. Yost and C. G. Enke, *Anal. Chem.*, 1979, **51**, 1251–1264.

26 F. W. McLafferty, J. Wiley and Sons, New York, NY, 1983, p. 22.

27 U. Chiluwal, G. Lee, M. Y. Rajapakse, T. Willy, S. Lukow, H. Schmidt and G. A. Eiceman, *Analyst*, 2019, **144**, 2052–2061.

28 H. Shokri, M. Vuki, B. D. Gardner, H. C. Niu, U. Chiluwal, B. K. Gurung, D. B. Emery and G. A. Eiceman, *Anal. Chem.*, 2019, **91**, 6281–6287.

29 M. Amo-Gonzalez, S. Perez, R. Delgado, G. Arranz and I. Carnicero, *Anal. Chem.*, , DOI:10.1021/acs.analchem.9b03589.

30 M. Amo-González, I. Carnicero, S. Pérez, R. Delgado, G. A. Eiceman, G. Fernández De La Mora and J. Fernández De La Mora, *Anal. Chem.*, 2018, **90**, 6885–6892.

31 H. Shokri, E. G. Nazarov, B. D. Gardner, H.-C. Niu, G. Lee, J. A. Stone, N. Jurado-Campos and G. A. Eiceman, *Anal. Chem.*, 2020, **92**, 5862–5870.

32 S. Kendler, G. R. Lambertus, B. D. Dunietz, S. L. Coy, E. G. Nazarov, R. A. Miller and R. D. Sacks, *Int. J. Mass Spectrom.*, 2007, **263**, 137–147.

33 X. An, G. A. Eiceman, J. E. Rodriguez and J. A. Stone, *Int. J. Mass Spectrom.*, 2011, **303**, 181–190.

34 M. Maziejuk, J. Puton, M. Szyposzyńska and Z. Witkiewicz, *Talanta*, 2015, **144**, 1201–1206.

35 D. M. Ruszkiewicz, C. L. P. Thomas and G. A. Eiceman, *Analyst*, 2016, **141**, 4587–4598.

36 P. Brown, P. Watts, T. D. Märk and C. A. Mayhew, *Int. J. Mass Spectrom.*, 2010, **294**, 103–111.

37 J. Langejuergen, M. Allers, J. Oermann, A. Kirk and S. Zimmermann, *Anal. Chem.*, 2014, **86**, 11841–11846.

38 A. Bohnhorst, A. T. Kirk, M. Berger and S. Zimmermann, *Anal. Chem.*, 2018, **90**, 1114–1121.

39 D. Morsa, V. Gabelica and E. De Pauw, *J. Am. Soc. Mass Spectrom.*, 2014, **25**, 1384–1393.

40 E. Krylov, E. G. Nazarov, R. A. Miller, B. Tadjikov and G. A. Eiceman, *J. Phys. Chem. A*, 2002, **106**, 5437–5444.

41 S. B. Hawthorne and D. J. Miller, *Appl. Spectrosc.*, 1986, **40**, 1200–1211.

42 J. V. Headley and A. G. Harrison, *Can. J. Chem.*, 1985, **63**, 609–618.

43 J. A. N. A. Herman, A. G. Harrison, A. G. Harrison, J. A. N. A. Herman and A. G. Harrison, .

44 M. L. Sigsby, R. J. Day and R. G. Cooks, *Org. Mass Spectrom.*, 1979, **14**, 556–561.

45 A. Bohnhorst, A. T. Kirk, Y. Yin and S. Zimmermann, *Anal. Chem.*, 2019, acs.analchem.9b00810.

46 G. A. Eiceman, E. G. Nazarov and J. E. Rodriguez, *Anal. Chim. Acta*, 2001, **433**, 53–70.

Table 1. Oxygen-containing volatile organic compounds and compensation voltages for product ions and for ions measured by tandem DMS with an active reactive stage. First level refers to ions arising directly from the product ion at comparatively low E/N. Second level fragments are observed with increased E/N and are thought to form sequentially from fragment ions formed in a first level.

Class	Chemical	Carbon Number	Compensation Voltage (V)			
			$M_2H^+(H_2O)_n$	$MH^+(H_2O)_n$	First Level Fragment Ion	Second Level Fragment Ion
Alcohols	1-Propanol	3	-1.3	-	-4.55	-6.35
	1-butanol	4	-0.5	-5.6	-4.5	-
	1-pentanol	5	0	-3.65	-	-6.35
	1-hexanol	6	0.45	-2.45	-4.55	-6.4
	1-heptanol	7	0.65	-1.45	-4.55	-6.3
	octanol	8	0.85	-0.85	-4.5	-6.25
	2-Propanol	3	-0.9	-	-4.65	-6.3
	Isobutanol	4	-0.25	-5.05	-4.65	-
	Cyclohexanol	6	0.4	-3.1	-	-
Acetates	Propyl Acetate	5	0.5	-2.05	-4.45	-
	Butyl Acetate	6	0.5	-1.5	-4.4	-
	Pentyl Acetate	7	0.9	-1	-4.45	-
	Hexyl Acetate	8	1.45	-0.7	-4.5	-
	Heptyl Acetate	9	1.65	-0.45	-4.5	-
	Octyl Acetate	10	1.6	-0.25	-4.55	-
	Nonyl Acetate	11	1.8	0.05	-4.4	-
	IsoPropyl Acetate	5	0.65	-1.8	-4.55	-
	IsoButyl Acetate	6	0.75	-1.3	-4.5	-
	IsoPentyl Acetate	7	0.9	-0.9	-4.45	-
	Vinyl Acetate	4	0	-3.4	-7.8	-
	Methyl Butyrate	5	0.75	-2.05	-	-
	sec-butyl acetate	6	0.75	-1.15	-4.4	-
	Ethyl Acrylate	5	0.5	-2.6	-3.9	-
Ketones	2-pentanone	5	0.1	-2.95	-6.4	-
	2-hexanone	6	0.45	-2.2	-6.35	-
	2-heptanone	7	0.7	-1.45	-	-
	2-octanone	8	1	-1	-	-
	2-nonanone	9	1.15	-0.65	-	-
	2-decanone	10	1.25	-0.55	-	-
	MIBK	6	0.8	-1.85	-6.25	-4.7
	Pinacolone	6	0.95	-1.2		-
Aldehydes	Butanal	4	-0.45	-3.85	-6.05	-
	Pentanal	5	0.05	-2.9	-3.75	-
	Hexanal	6	0.3	-2.05	-2.6	-5.95
	Heptanal	7	0.45	-1.3	-1.7	-6.05
	Octanal	8	0.65	-1	-	-3.8
	Nonanal	9	0.8	-0.75	-	-3.7
Ethers	Diethyl Ether	4	0.15	-4.05	-	-6.4
	Dipropyl Ether	6	0.65	-1.5	-5	-6.35
	Dibutyl Ether	8	1.1	-0.4	-4.55	-6.35
	Dipentyl Ether	10	1.15	0.2	-3.7	-6.4
	Dihexyl Ether	12	1.45	0.4	-	-
	Diisopropyl Ether	6	0.8	-1.4	-4.45	-6.2

Table 2. Distribution of ions (by percentage, normalized to total intensity of product ions at 0 Td) from FIF Spectra for n-hexanal.

Td	$M_2H^+(H_2O)_n$	$MH^+(H_2O)_n$	Unsaturated carbocation	$C_4H_7^+$	Sum of intensity for product ions
0	30%	70%			100%
93	20%	60%			80%
103	19%	39%	17%		74%
113	15%	12%	45%		72%
124	9%		36%	3%	49%
134			22%	13%	36%
144			12%	12%	24%
155			7%	9%	16%

Table 3. Percent change of mass-analysed product ions for alcohols, aldehydes, and esters with active reactive stage and both DMS in all ion pass. Values were adjusted for background abundances from ion fragmentation in the vacuum interface. See Table 1 legend.

Compounds	Proton Bound Dimer	Protonated Monomer	First Level Fragment Ion		Second Level Fragment Ion	
Alcohols	$M_2H^+(H_2O)_n$	$MH^+(H_2O)_n$	(MH^+)-H_2O	(MH^+)-H_2	$C_5H_{11}^+$	$C_4H_9^+$
1-Propanol	-28%	1%	-3%	28%	-	-
1-butanol	-1%	-14%	14%	-	-	-
1-pentanol	-3%	-14%	15%	-	-	-
1-hexanol	4%	-15%	14%	-	-	-
1-heptanol	13%	-18%	-5%	-	-	12%
1-octanol	8%	-16%	-1%	-	3%	7%
2-Propanol	-10%	-2%	-3%	17%	-	-
Isobutanol	-22%	8%	20%	-	-	-
2-butanol	-29%	9%	23%	-	-	-
Cyclohexanol	-14%		28%	-	-	-
Aldehydes	$M_2H^+(H_2O)_n$	$MH^+(H_2O)_n$	Unsaturated carbocation		$C_5H_9^+$	$C_4H_7^+$
Butanal	-24%	4%	20%	-	-	-
Pentanal	-15%	-17%	31%	-	-	-
Hexanal	-1%	3%	-14%	-	-	12%
Heptanal	17%	-26%	6%	-	-	4%
Octanal	2%	-28%	16%	-	6%	-
Nonanal	8%	-26%	11%	-	4%	-
Esters	$M_2H^+(H_2O)_n$	$MH^+(H_2O)_n$			$C_2H_4O_2H^+$	$C_3H_4O_2H^+$
Propyl Acetate	-27%	-11%	-	-	37%	-
Butyl Acetate	2%	-17%	-	-	18%	-
Pentyl Acetate	-35%	2%	-	-	29%	-
Hexyl Acetate	10%	-16%	-	-	8%	-
Heptyl Acetate	12%	-14%	-	-	3%	-
Octyl Acetate	12%	-16%	-	-	4%	-
Nonyl Acetate	22%	-24%	-	-	2%	-
IsoPropyl Acetate	-24%	-15%	-	-	38%	-
IsoButyl Acetate	-9%	-15%	-	-	16%	-
IsoPentyl Acetate	15%	-17%	-	-	-	-
Vinyl Acetate	-28%	-17%	-	-	54%	-
Methyl Butyrate	-11%	11%	-	-	-	-
sec-Butyl Bcetate	-10%	-22%	-	-	31%	-
Ethyl Acrylate	-20%	-30%	-	-	-	48%

LIST OF FIGURES

Figure 1. Fowler, et al

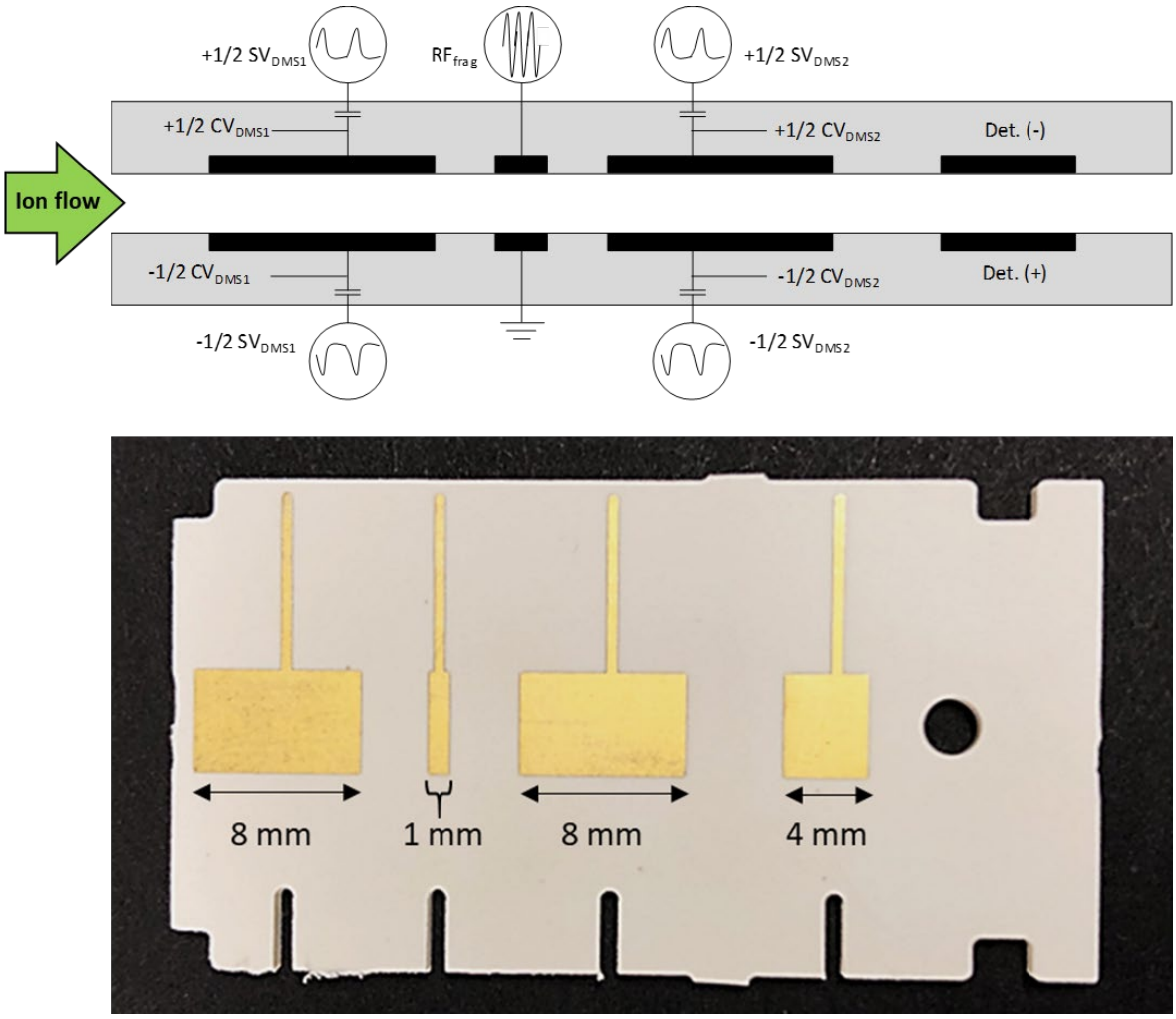

Figure 2. Fowler, et al

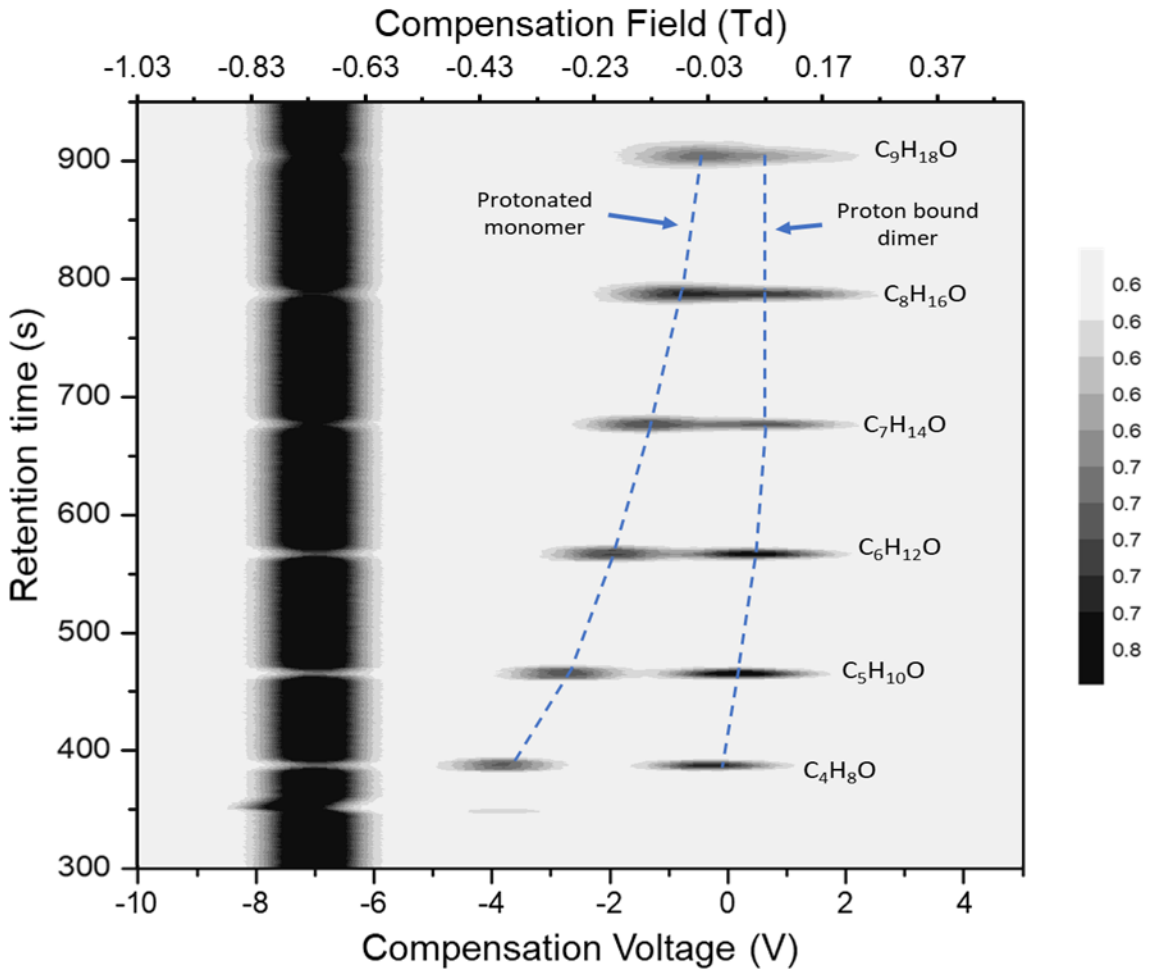

Figure 3. Fowler, et al

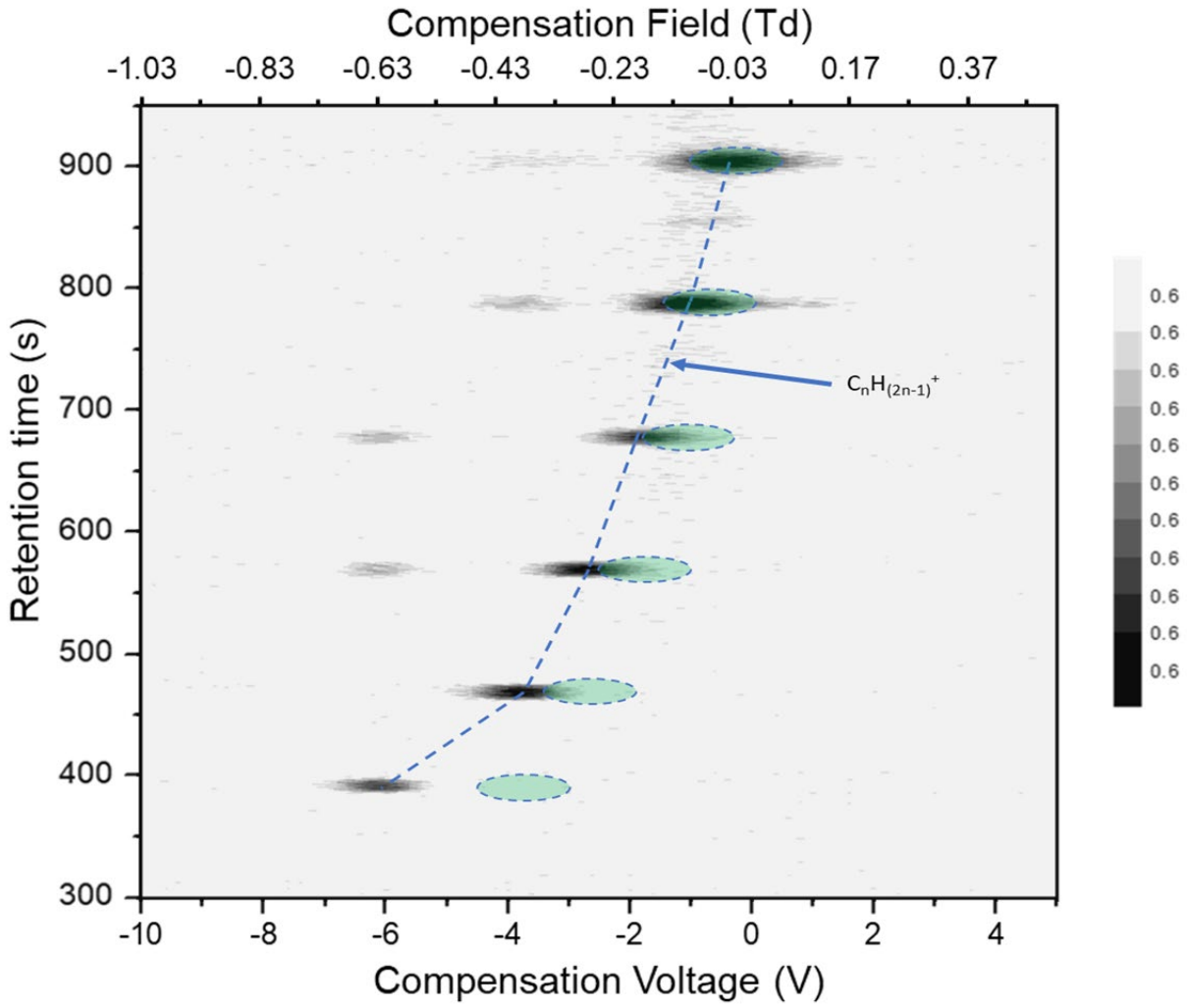

Figure 4

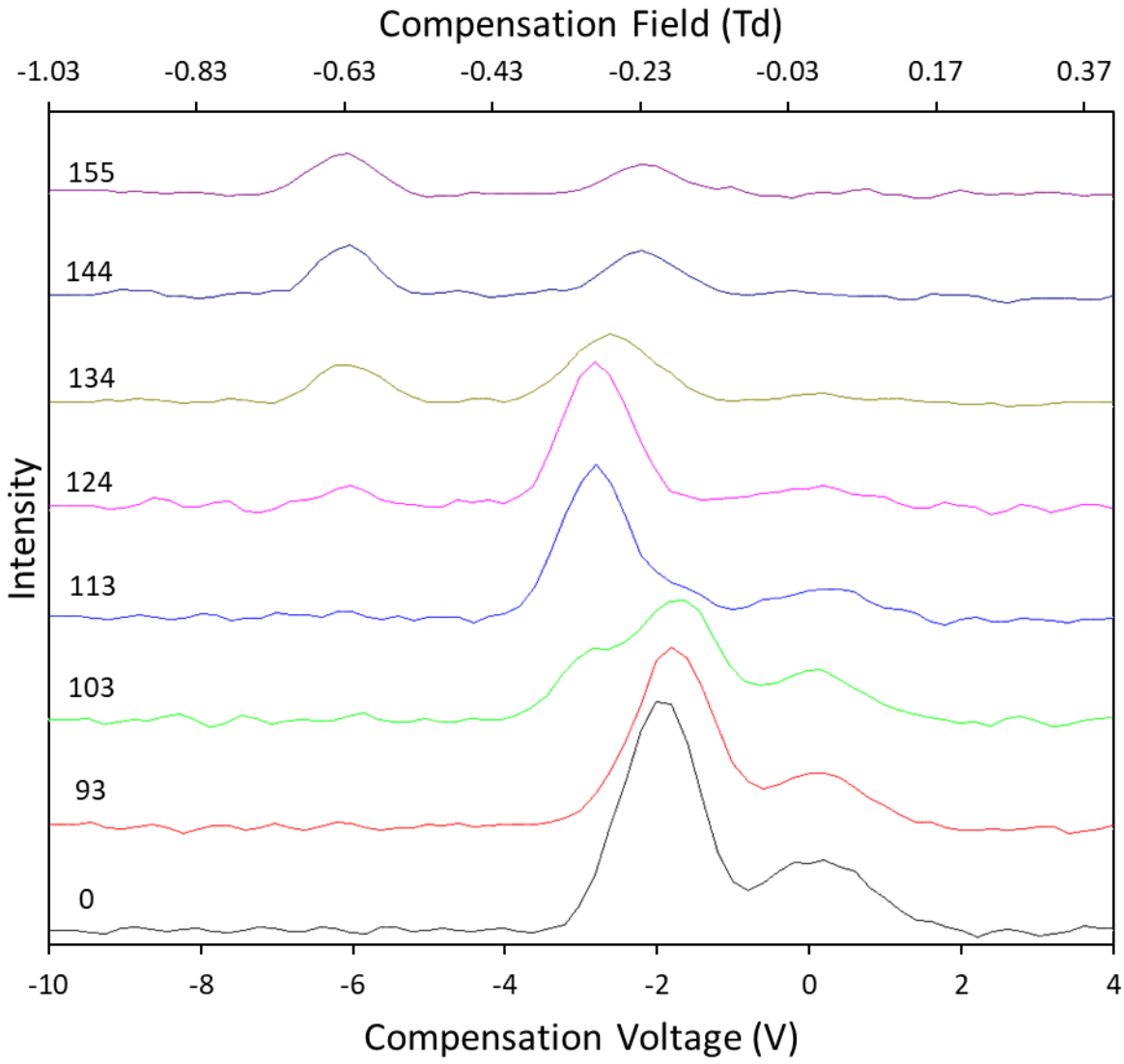
Compensation Field (Td)
-1.03
-0.83
-0.63
-0.43
-0.23
-0.03
0.17
0.37
155
144
134
124
113
103
93
0
Intensity
-10
-8
-6
-4
-2
0
2
4
Compensation Voltage (V)

Figure 5. Fowler, et al

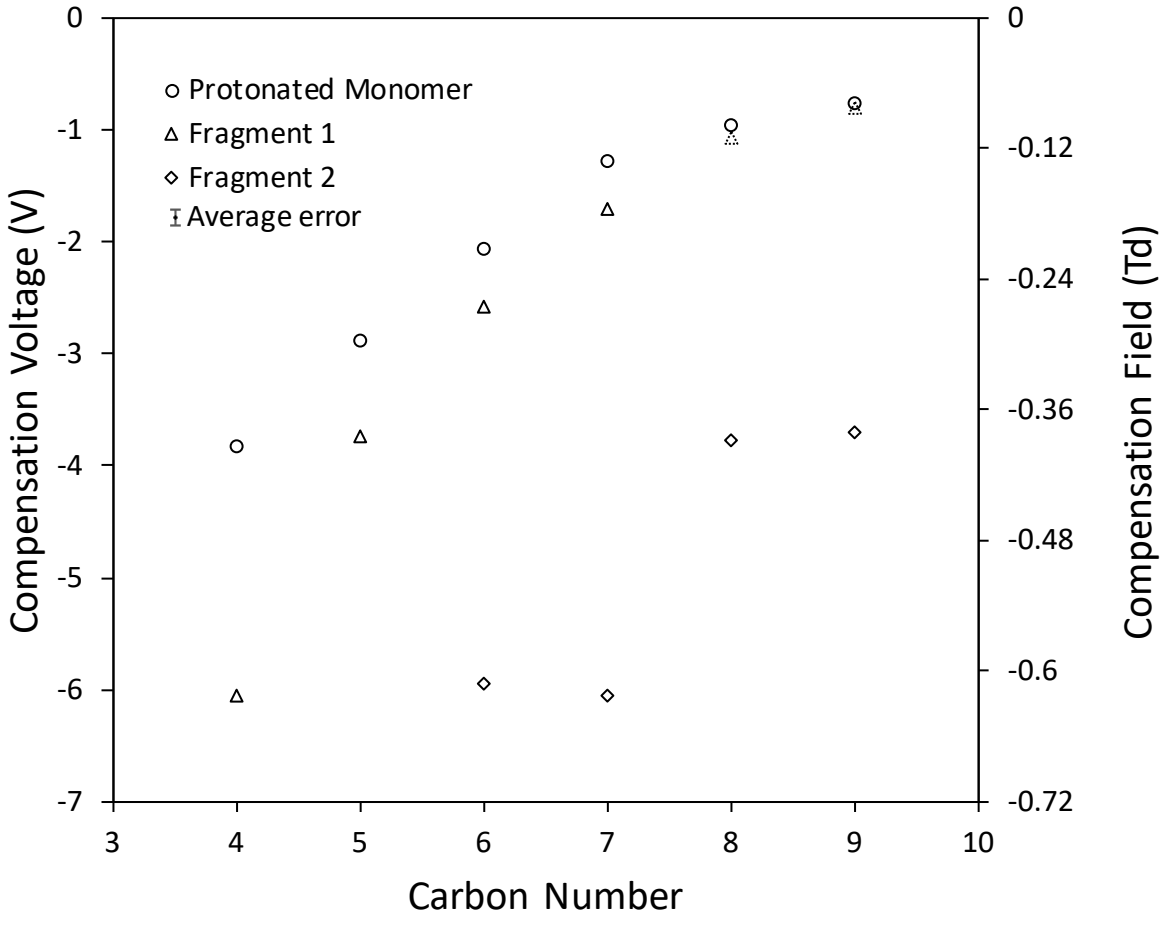

Figure 6. Fowler, et al

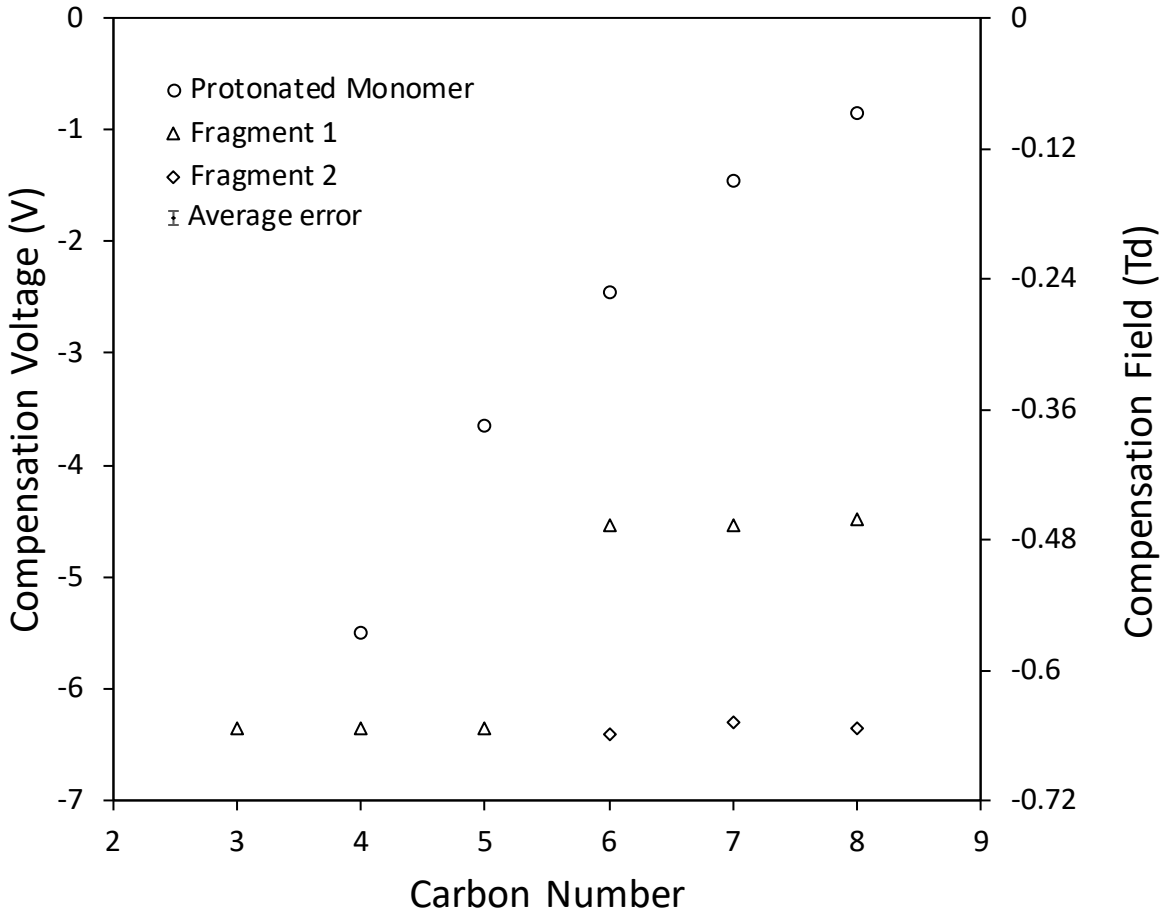

Figure 6. Fowler, et al

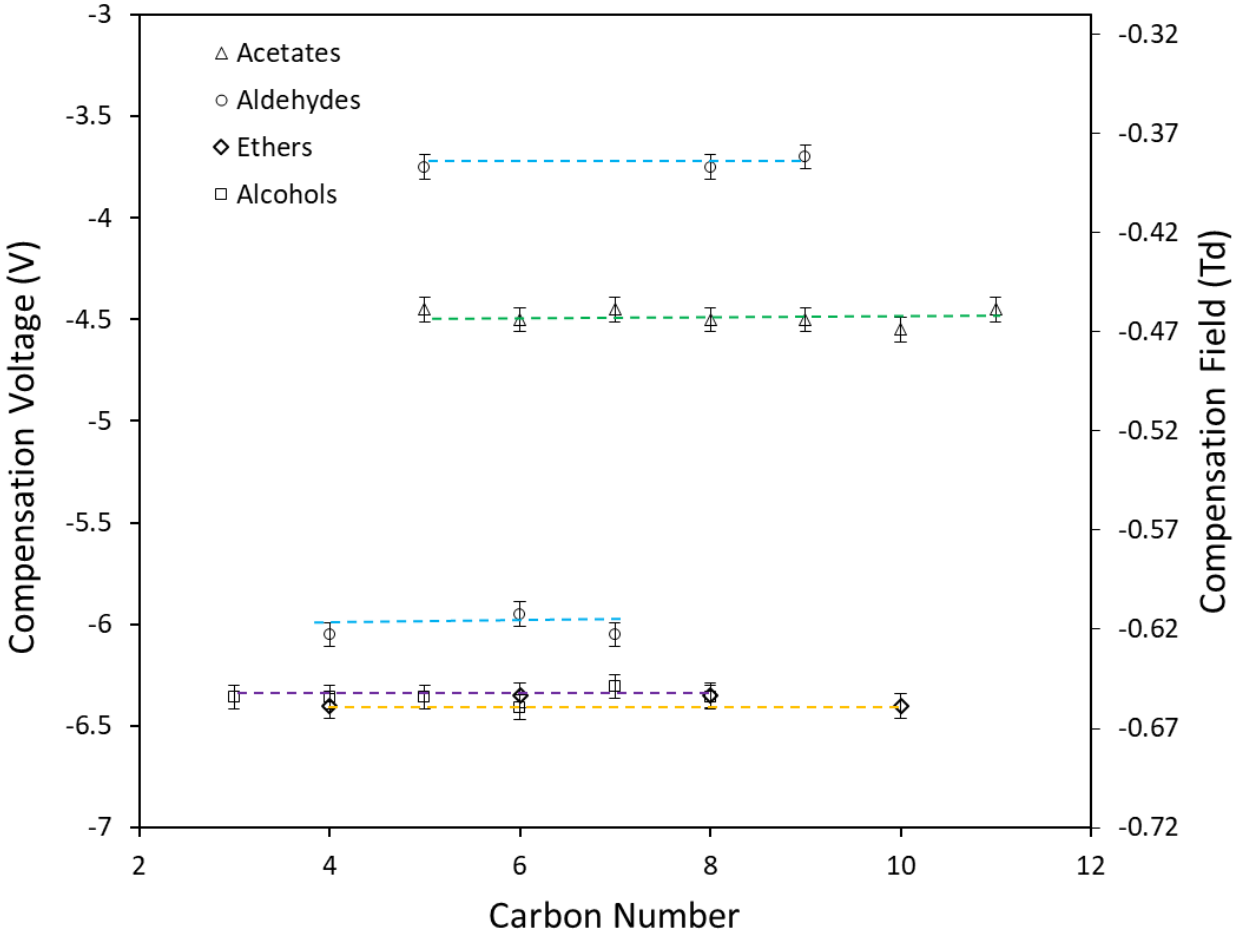

Figure 7. Fowler, et al

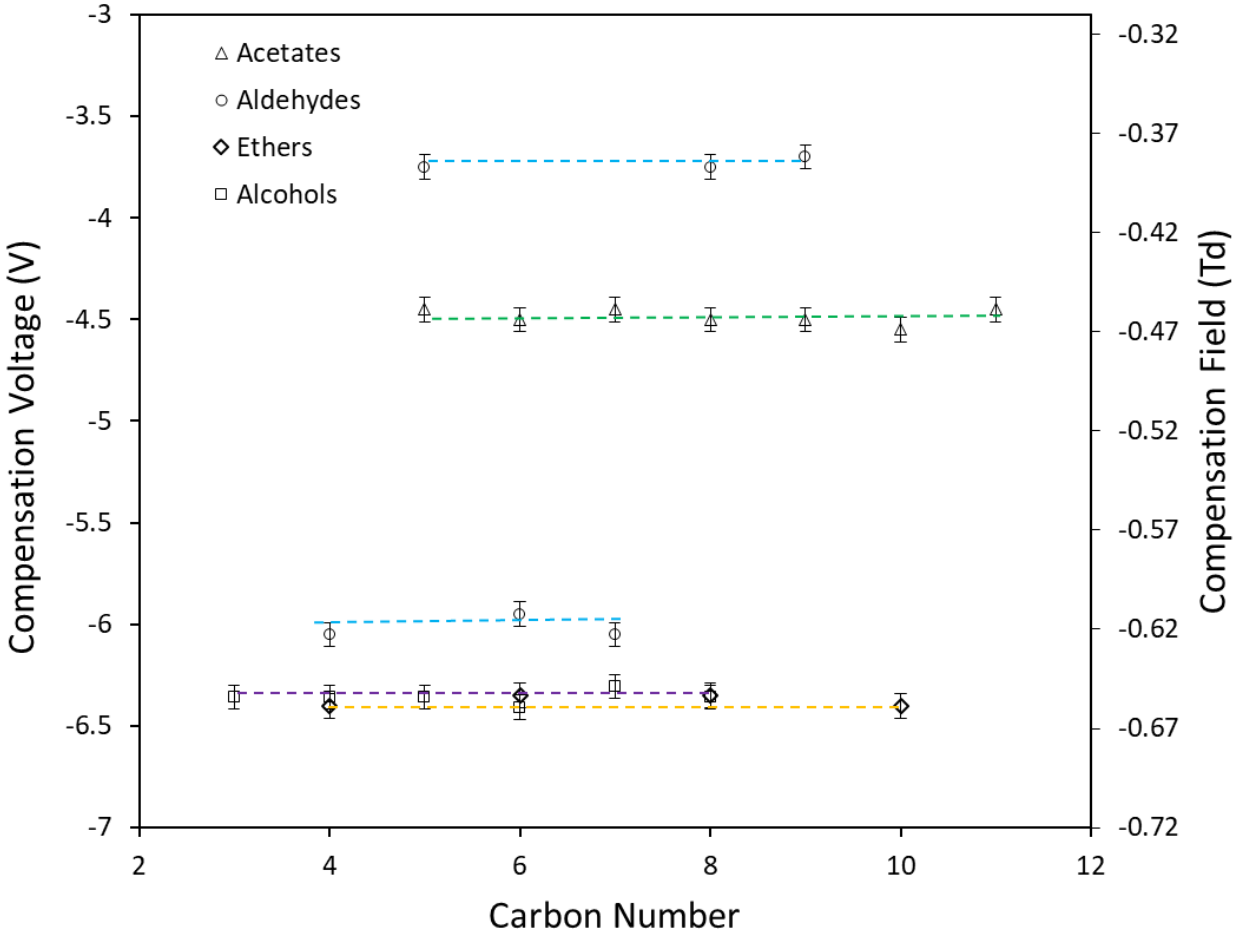

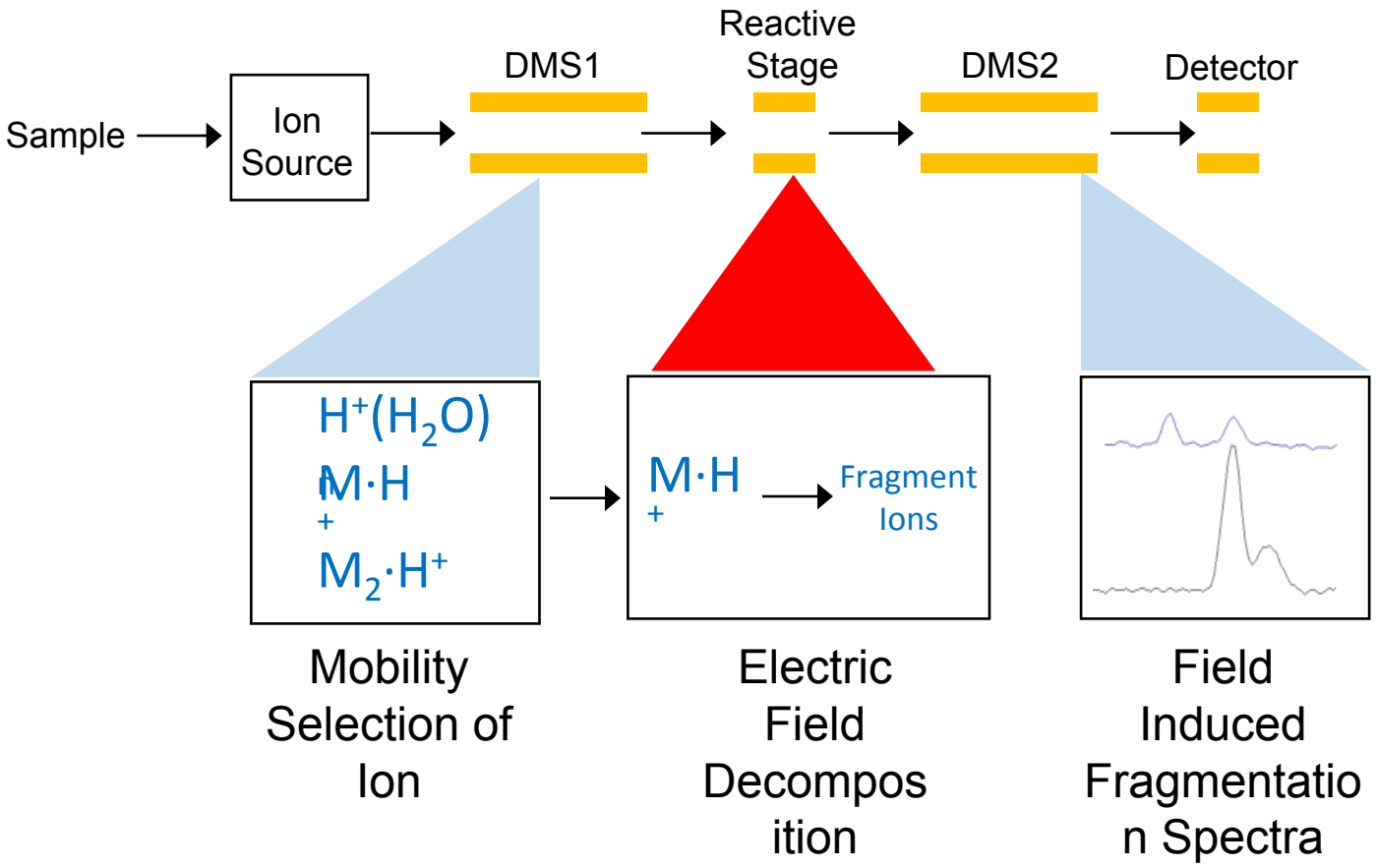
Sample
Ion Source
DMS1
Reactive Stage
DMS2
Detector
$H^+(H_2O)$
$M \cdot H^+$
$M_2 \cdot H^+$
$M \cdot H^+$
Fragment Ions
Mobility Selection of Ion
Electric Field Decomposition
Field Induced Fragmentation Spectra